ECOLOGY *Letters*, (1998) **1**: 63–70

REPORT

Cities and villages: infection hierarchies in a measles metapopulation

B.T. Grenfell[1] and B.M. Bolker[2]
[1]Zoology Department, Cambridge University, Downing Street, Cambridge CB2 3EJ, UK. E-mail: bryan@zoo.cam.ac.uk
[2]Department of Ecology and Evolutionary Biology, Princeton University, Princeton, NJ 08544–1003, USA.

Abstract

An important issue in the dynamics of directly transmitted microparasites is the relationship between infection probability and host density. We use models and extensive spatio-temporal data for the incidence of measles to examine evidence for spatial heterogeneity in transmission probability, in terms of urban–rural hierarchies in infection rate. Pre-vaccination measles data for England and Wales show strong evidence for urban–rural heterogeneities in infection rate – the proportion of urban cases rises significantly before major epidemics. The model shows that this effect is consistent with a higher infection rate in large cities, though small towns have epidemic characteristics intermediate between town and country. Surprisingly, urban and rural areas of the same population size have a similar propensity for local extinction of infection. A spatial map of urban–rural correlations reveals complex regional patterns of synchronization of towns and cities. The hierarchical heterogeneities in infection persist into the vaccine era; their implications for disease persistence and control are discussed.

Keywords

Correlation, epidemiology, heterogeneity, infection dynamics, measles, metapopulation, microparasite, vaccination.

Ecology *Letters* (1998) 1: 63–70

INTRODUCTION

A key debate in microparasite ecology centres on the scaling relationship between host population density and parasite transmission rate (Greenwood *et al.* 1936; Kermack & MacKendrick 1939; Anderson & May 1979, 1991; Dietz 1982; May & Anderson 1985; de Jong *et al.* 1995). The way in which *per capita* host infection rate scales with their population size and/or density has a profound impact, both on the dynamics and persistence of epidemics (Grenfell & Dobson 1995) and on the prospects for their control (Anderson & May 1991).

The issue of spatial heterogeneity and control has crystallised around the ''cities and villages'' models of Anderson and May (May & Anderson 1984; Anderson & May 1991). These models explore the implications for vaccination strategies against childhood infections when transmission rates are lower in rural areas than in towns. Childhood infections, in particular measles, have been a fruitful area for the synthesis of models and epidemiological time series (as reviewed by Anderson & May 1991; Grenfell & Harwood 1997). The most important manifestation of population size is the local extinction of measles in urban populations below a Critical Community Size of 250,000–400,000 (Bartlett 1957, 1960). Regional studies of measles spatial dynamics also indicate that infection diffuses from urban centres to surrounding rural areas (Cliff *et al.* 1993). However, the urban–rural hierarchy has not been analysed on the large spatial and long temporal scales provided by measles notifications in developed countries.

Here, we present an analysis of urban–rural infection hierarchies, based on a uniquely detailed spatio-temporal data set, for measles in England and Wales. Comparison of empirical patterns and epidemiological models indicates significantly higher urban infection rates, especially in large towns. These results have implications both for the spatio-temporal dynamics and for the persistence of infection and the design of vaccination strategies.

METHODS

Data set and preliminary analysis

We use weekly measles notifications and associated demographic data for England and Wales (Grenfell &

Harwood 1997; Keeling & Grenfell 1997). For the pre vaccination era, before 1967, measles case data are available for 845 cities and towns and 457 rural districts. In the vaccine era, boundary changes make the urban–rural division more difficult, so that we use data for the 60 largest towns and cities for the urban aggregate and the remainder as an approximation to the rural total.

A plot of the aggregate urban and rural pre vaccination time series (Fig. 1a) indicates the well-known synchronous, biennial dynamics (Fig. 1c) of measles before vaccination in England and Wales (Fine & Clarkson 1982; Schenzle 1984; Grenfell *et al.* 1994). The urban epidemics lead the rural ones slightly. We explore this by superimposing the time series of proportional cases in towns on the overall case totals (Fig. 1b). This reveals a much sharper distinction – the proportion of urban cases peaks markedly before the main epidemic. Standard time series analysis (Fig. 1c) confirms this picture, as a highly significant peak cross-correlation between the cases and urban proportions lagged by around 12 weeks.

This lagged pattern is summarized in Fig. 2(a), which shows the mean pre vaccination biennial pattern of cases and urban proportions. *How could such a pattern arise?* The main epidemic starts in week 40 of the biennium; this corresponds to the start of the Autumn school terms and reflects the importance for measles dynamics of seasonality in transmission, driven by relatively high contact rates of children in schools (Fine & Clarkson 1982). The proportion of urban cases rises before this time, then declines sharply during the main epidemic. This suggests more intense transmission of infection in towns compared with rural areas.

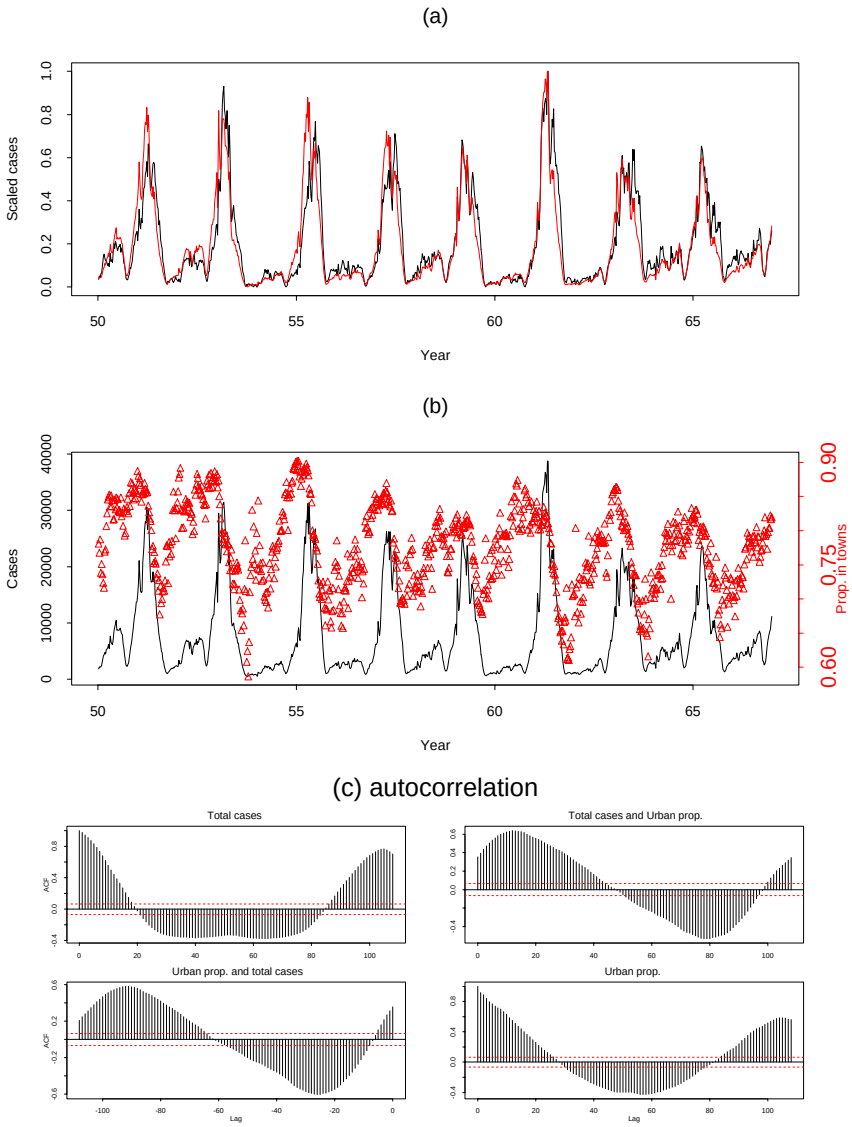

Figure 1 (a) Rural (black) and urban (red) time series of weekly measles notifications for England and Wales, 1950–67. This period provides the most regular biennial epidemics of the prevaccination era, and so is used for subsequent analyses. (b) Corresponding total case time series (black) and proportion in the urban aggregate (red). (c) Auto-and cross-correlations for the series in (b) (Chatfield 1975). The top left graph shows the autocorrelation pattern of total cases, as a function of a copy of the series at the specified lag (weeks); the bottom right figure repeats this for the time series of proportion in towns. The off-diagonal graphs show the cross-correlation between series; the upper right shows positive lags (leads) for proportion of cases, the lower left negative lags. The red lines are 99% confidence intervals for zero correlation.

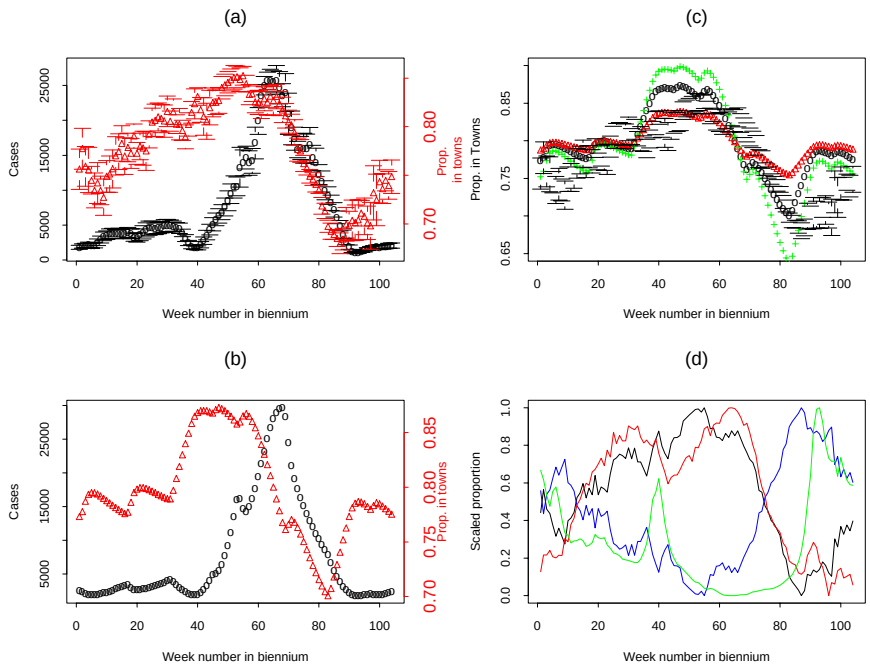

Figure 2 (a) Average biennial pattern (with standard errors) for the total aggregate measles cases and urban proportions (red) of Fig. 1(b). (b) Equivalent results for a deterministic realization of the two-patch age-structured SEIR model described in the text – full details of this Realistic Age Structured (RAS) model are given by Bolker & Grenfell (1993). Patch sizes are equated in size to the urban and rural population aggregates; the results are not affected strongly across the realistic range of cross-coupling in infection (Bolker & Grenfell 1995); we used $\varepsilon = 1\%$. As described in the text, the model assumes an urban/rural ratio in the average infection parameter of $a = 1.5$. (c) Urban biennial patterns for simulations using different values of a (1.2, red; 1.5, black; 1.8, green) illustrates that $a = 1.5$ gives the best least squares fit to the observed proportion (error bars). (d) Observed mean biennial pattern of cases (scaled on {0, 1}) in all urban centres (black), cities above a population of 250,000 (red), the rural aggregate (blue), and small towns (<30,000 population size; green); for clarity, error bars are not shown.

Epidemiological models

We explore this with a simple model, based on the standard SEIR compartmental framework (Anderson & May 1991), when two populations are epidemiologically coupled (Grenfell *et al.* 1995):

$$\textit{Susceptible}\quad \frac{dS_i}{dt} = \mu(N_i - S_i) - [\beta_i I_i + \varepsilon\beta_j I_j]\frac{S_i}{N_i}$$

$$(i = 1, 2;\ j \neq i)$$

$$\textit{Exposed}\quad \frac{dE_i}{dt} = [\beta_i I_i + \varepsilon\beta_j I_j]\frac{S_i}{N_i} - (\mu + \sigma)E_i$$

$$\textit{Infectious}\quad \frac{dI_i}{dt} = \sigma E_i - (\mu + \gamma)I_i$$

Here, we have assumed that both populations ($i = 1, 2$) have constant population size (N) and population turnover (birth, death) rate, μ; only the rate equations for S, E, and I are therefore necessary to describe the system's dynamics (Anderson & May 1991). Susceptibles (S_i) in patch i are replenished by births, and depleted by infection, through contact with infectives (I). The infection process within patch i is controlled by a *per capita* infection parameter, β_i, with a cross-infection rate from infectives in patch j determined by a coupling proportion, ε. Infected individuals move into a non infectious exposed class (E) for $1/\sigma$ days and are then infectious for an average of $1/\gamma$ days. We use the parameter estimates $\mu = 0.013$/year, $\sigma = 48.67$/year, $\gamma = 56.19$/year (Olsen *et al.* 1988), with a default cross-coupling proportion, $\varepsilon = 0.01$ (Bolker & Grenfell 1995).

In practice, we adopt a standard age-structured formulation of this model, which allows seasonal increases in the infection rate during school terms (Schenzle 1984). The structure of the model and associated estimates of the infection parameters are documented fully by Bolker & Grenfell (1995, 1996).

RESULTS

The model (Fig. 2b) is a close fit to the observed biennial pattern of pre vaccination measles epidemics (Fig. 2a) (Schenzle 1984; Bolker & Grenfell 1995, 1996; Ferguson *et al.* 1996; Keeling & Grenfell 1997). Figure 2 (b) also shows the expected proportion in cities (patch 1), from our two patch model. We assume that patches 1 and 2 correspond to the urban and rural aggregates, respectively, with a higher infection rate in the urban centres (i.e. $\beta_1 = a\beta_2$, $a > 1$). An urban–rural difference of around 50% ($a = 1.5$) provides the best least squares fit to the observed biennial fraction in towns (Fig. 2c).

Comparing the observed (Fig. 2a) and expected (Fig. 2b) urban proportions indicates a close fit of our simple model. The simulation overestimates the rise of the epidemic at the start of the school term, but otherwise captures the difference in timing between urban and rural epidemics very closely. In reality, of course, the urban and rural areas are coupled locally, rather than as aggregates. Nevertheless, the model indicates that the aggregates act as though towns and cities experience a significantly higher average measles infection rate than the rural hinterland.

This result parallels, at a national level, work in spatial geography, which indicates an urban–rural infection hierarchy in regional measles epidemics (Cliff & Haggett 1988; Cliff *et al.* 1993). A conclusion of the latter studies was that local extinction of measles below the critical community size would also influence the hierarchical spread of infection.

We explore this in Fig. 2(d), which shows the observed biennial proportion of cases in large cities and small towns, compared with the urban and rural aggregates. Unsurprisingly, large cities follow the pattern of early epidemic onset of the urban total. By contrast, the proportion in small towns (population size up to 30,000) is much closer to the rural pattern – a later onset of the major epidemic. However, both small and large urban centres are distinct from the rural aggregate in showing a spike in relative cases at the start of the major epidemic in week 40 (Fig 2d).

Small towns therefore seem to exhibit both urban and rural characteristics in the timing of epidemics. They also tend to show highly irregular epidemic patterns (Bartlett 1957; Grenfell 1992; Cliff *et al.* 1993; Rhodes & Anderson 1996), with significant local extinction (fadeout) of infection in the troughs between epidemics.

This result raises the question whether the apparent difference in urban and rural infection rates is due to a greater tendency for rural areas to lose infection (with a subsequent lag in its reintroduction).

We examine this in Fig. 3, which shows the pattern of local "fadeout" (extinction of infection), as a function of population size, for urban (red) and rural (green) areas. The prevaccination extinction pattern is shown in two ways. First, the total period of extinction declines approximately linearly with log(population size) (Bartlett 1960). Second, the *number* of extinctions shows a peak at intermediate population size. This reflects a trend from few, long extinctions in very small populations, via many short fadeouts at intermediate population size, to few

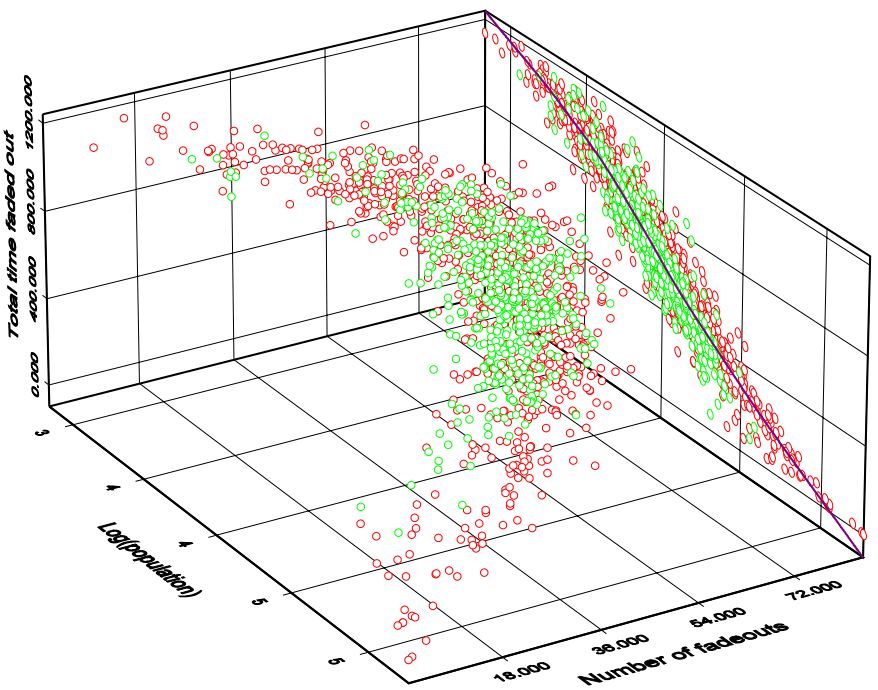

Figure 3 Pattern of fadeouts of infection (> 2 weeks without cases; Bartlett 1960) in towns (red) and rural areas (blue). The three-dimensional cloud shows total length of fadeout in the prevaccination era, plotted against log(population size) and number of fadeouts. The projection on the population, total fadeouts axis is fitted with a standard lowess nonparametric curve.

short ones in the inter epidemic period of larger communities, near the critical community size. Surprisingly, Fig. 3 shows that both these patterns are similar for urban and rural areas, which are therefore not distinctively different in their propensity for extinction.

Patterns of spatial synchrony

The aggregate patterns presented so far ignore the explicit local spatial diffusion of measles from towns to the rural hinterland (Cliff *et al.* 1993). As a first step in this direction, we therefore explore the correlation between the rural aggregate time series and the proportion of total (urban and rural cases) in each urban centre. This (unlagged) correlation gives a simple necessary condition for the proportion of cases in a given town or city to rise consistently ahead of the aggregate rural epidemic. The relationship between this measure of urban–rural correlation and urban population size is shown in Fig. 4(a). Essentially, large cities such as London and Birmingham tend to have a strong negative correlation, reflecting the relative increase in measles in these centres before the start of the rural epidemic (Fig. 2d). As shown in Fig. 4(a), Liverpool is an exception to this – its correlation with the rural aggregate is almost zero. This is due to the distinctive pre vaccination measles dynamics in Liverpool, where high birth rates drove the epidemic at a relatively fast rate (Finkenstädt & Grenfell 1998; Finkenstädt *et al.* 1998). The resulting strongly annual epidemic pattern has a relatively low correlation with the biennial pattern of the rural aggregate.

At the other extreme of population size, the proportion of cases in very small centres have a correlation near zero with the rural aggregate, reflecting their irregular pattern of epidemics. For intermediate population sizes, the variance of the correlation between relative urban cases reaches a maximum. This pattern is explored in Fig. 4(b), which maps the correlations spatially. This reveals a clear clustering of medium sized towns that are negatively correlated with the rural aggregate (the green points). The main focus is in the North-west (around Manchester), the North-east (around Newcastle), and Birmingham – surprisingly, there is no focus of correlation around London. The clustering of negative correlations in the North-west implies that the timing of epidemics, relative to the rural aggregate, for small centres in this high density region are regionally synchronized with large cities, such as Manchester and Leeds. More generally, this result suggests that the spatial pattern of effective infection rate in the disease metapopulation depends on regional coup-ling as well as local population density. Analysing such patterns fully will require explicitly considering the pattern of urban–rural correlation on a local and regional scale.

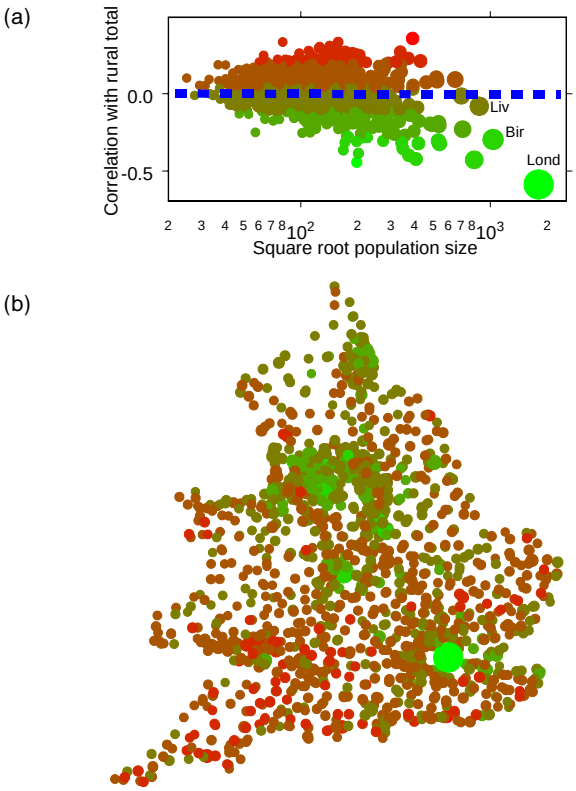

Figure 4 Spatial patterns of synchrony between urban measles time series and the rural aggregate. We plot correlations of the rural total against proportional cases for each urban location (cases in location i/total urban and rural cases). We use simple (zero lag) Pearson correlation for each of the 845 towns and cities in the data base; experiments (not shown) indicate that a strong nega-tive correlation is a reasonable simple index of a lag between the rise in pro-portional cases in a town and the subsequent start of the rural epidemic (note that this is a different correlation from the urban proportion-total cases correlation shown in Fig. 1). (a) Correlation as a function of urban population size. Square root (Population size) is shown (on a log scale; x axis) to correspond with the symbol size (area is proportional to population). The correlation (y axis) is also coded as symbol colour (red, maximum; green, miminum). Significance of the correlations is measured by the blue dashed line; the thickness of the line gives an approximate 1% confidence limit for a correlation coefficient of zero, corrected for multiple tests with a Bonferroni correction. Even after correcting for 845 tests (critical $\alpha = 0.000012$), most correlations are significantly different from zero, because each correlation is based on 830 xy pairs. (b) The same data plotted on a map of England and Wales.

The vaccine era

Theory tells us that relatively high average infection rates in large urban centres have important implications for the design of vaccination strategies (May & Anderson 1984). This heterogeneity should again translate into a lag

between the proportion of cases in large urban centres and the overall time series of cases. Figure 5 explores this relationship for the vaccination era. For comparison with the pre vaccination results, we focus on the period 1972–80, when epidemic patterns were still relatively stable. Urban and rural cases are not disaggregated for these data, so that we compare the cases in large cities with the total.

Vaccination reduces the biennial component of epidemics (Fig. 5a) (Anderson & May 1991) and greatly increases their variability (Bolker & Grenfell 1996). This variation is also apparent in the time series of large city case proportions. However, the lag between total cases and the proportion in cities is again apparent. This is confirmed by autocorrelation analysis (Fig. 5b), which shows significant peak cross-correlations at a 6 month lag.

DISCUSSION

This analysis reveals significant differences in the timing of measles epidemics in urban and rural aggregates in England and Wales, both before and since the onset of mass vaccination. We use a simple model to indicate that these results are remarkably consistent with a significantly higher contact rate between infectives and susceptible individuals in urban centres. Overall, this is compatible with the cities and villages paradigm (May & Anderson 1984; Anderson & May 1991), that the average force of infection is concentrated in large urban centres. The analysis presented here shows evidence for this heterogeneity in the dynamics of epidemics.

On an ecological front, our results imply a hierarchy of infection from large, high density host populations to smaller, low density units (Cliff & Haggett 1988). However, there are two *caveats* attached to this conclusion. First, our analysis considers aggregate rural dynamics and does not address the spatial diffusion of epidemics explicitly. An interesting possibility for future work here is to estimate population density explicitly for all areas and relate it to model estimates of the infection parameter. This is likely to be feasible for the relatively regular epidemics in large centres (Finkenstädt & Grenfell 1998); however, the irregular epidemic sequence in small centres presents a greater challenge for modelling.

The second complication arises from the behaviour of small towns, which show a mixture of urban and rural characteristics in the timing of epidemics. This reinforces the conclusion of Cliff & Haggett (1988, 1993) that epidemics diffuse from large centres – where the infection is endemic – both to small towns and to rural districts. The preliminary spatial analysis in Fig. 4 reinforces this point. The correlation map implies that the measles metapopulation dynamics in small centres – where infection frequently fades out in epidemic troughs – may depend on the

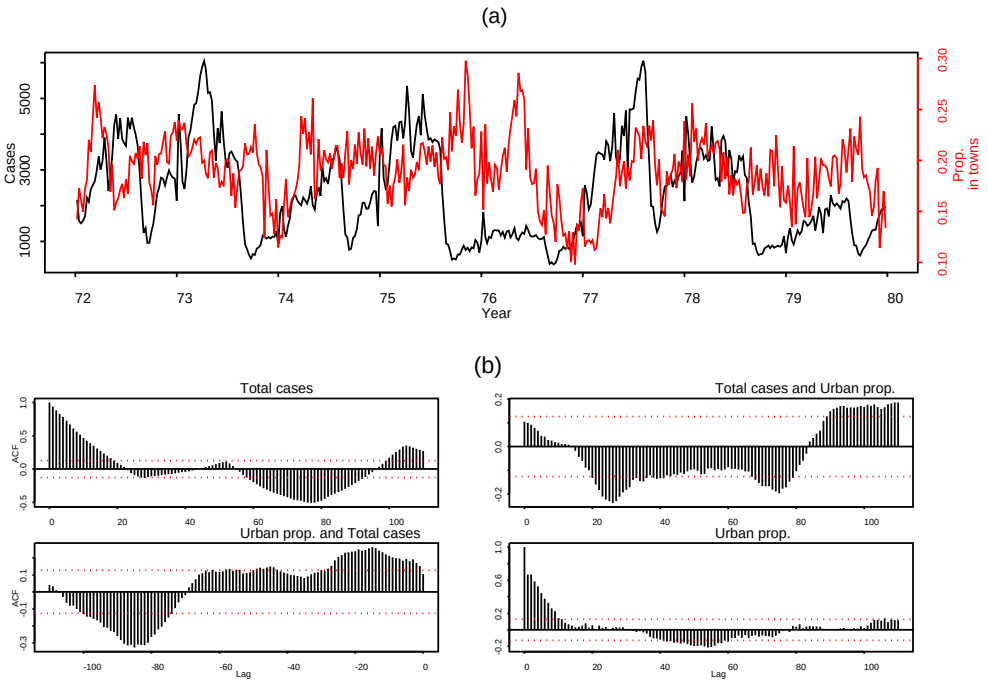

Figure 5 (a) Total time series of case and urban proportion during 1972–80. (b) Auto-and cross-correlations for these series, as described in Fig. 1.

hierarchy of contacts to larger centres (Finkenstädt & Grenfell 1998). These results also indicate considerable regional and local spatio-temporal correlation structure (and surprising lack of structure around London). To separate this effect from contact rate heterogeneities, we shall again require a more detailed spatially explicit analysis of the local and regional diffusion of epidemics. Figure 4 illustrates that factoring out the overall epidemic pattern, by expressing local cases as proportions of the total time series, may provide novel perspectives on these patterns.

The pattern of fadeout of infection in epidemic troughs is especially sensitive to the degree of coupling to large centres (Finkenstädt & Grenfell 1998). Surprisingly, we find that the overall fadeout profile does not differ markedly for urban and rural areas of the same size. Along with the synchrony of prevaccination dynamics between urban and rural areas (Fig. 1a), this illustrates the combined power of seasonal forcing (Grenfell *et al.* 1995) and epidemiological coupling in correlating the overall prevaccination dynamics of measles in England and Wales.

The vaccine era presents a different picture. Vaccination has acted to de-synchronize epidemics in different cities (Cliff *et al.* 1992; Bolker & Grenfell 1996) and this is reflected in the epidemic variations shown in Fig. 4. The proportion of cases in large towns and cities is out of phase with the aggregate epidemic pattern, so that it predominates in the inter epidemic period. This is potentially very significant, because it implies that large centres act as more of a reservoir of infection for the disease metapopulation in the vaccine era. This reservoir effect will be magnified by the observed decorrelation of measles epidemics in the vaccination era (Bolker & Grenfell 1996).

This finding has implications for the focus of vaccination efforts in large centres (May & Anderson 1984; Anderson & May 1991) and for future theoretical work on spatial vaccination strategies which aim to synchronize epidemic troughs (Earn *et al.* 1998; Grenfell & Harwood 1997). In particular, our analysis indicates that concentrating vaccination on large centres could have the added benefit of offsetting their role as reservoirs of infection in epidemic troughs, apparent in Fig. 4. This effect arises from a stochastic property of the measles metapopulation, superimposed on the deterministic threshold underpinning the cities and villages effect.

More broadly, this analysis underlines the suitability of childhood infections as a model for spatial heterogeneity and metapopulation dynamics.

ACKNOWLEDGEMENTS

We thank David Earn, Barbel Finkenstädt, Matt Keeling and Pej Rohani for helpful comments. BG was supported by the Wellcome Trust and BMB by Paul Mellon.

REFERENCES

Anderson, R.M. & May, R.M. (1979). Population biology of infectious diseases: Part I. *Nature*, 280, 361–367.

Anderson, R.M. & May, R.M. (1991). *Infectious Diseases of Humans: Dynamics and Control.* Oxford: Oxford University Press.

Bartlett, M.S. (1957). Measles periodicity and community size. *J. Roy. Statist. Soc. Ser. A*, 120, 48–70.

Bartlett, M.S. (1960). The critical community size for measles in the U.S. *J. Roy. Statist. Soc. Ser. A*, 123, 37–44.

Bolker, B.M. & Grenfell, B.T. (1993). Chaos and biological complexity in measles dynamics. *Proc. Roy. Soc. London, Ser. B*, 251, 75–81.

Bolker, B.M. & Grenfell, B.T. (1995). Space, persistence and the dynamics of measles epidemics. *Philosoph. Trans. Roy. Soc. London, Ser. B-Biol Sciences*, 348, 309–320.

Bolker, B.M. & Grenfell, B.T. (1996). Impact of vaccination on the spatial correlation and dynamics of measles epidemics. *Proc. Nations Acad. Sci. USA*, 93, 12648–12653.

Chatfield, C. (1975). *The Analysis of Time Series: Theory and Practice.* London: Chapman & Hall.

Cliff, A.D. & Haggett, P. (1988). *Atlas of Disease Distributions: Analytic Approaches to Epidemiologic Data.* Oxford: Basil Blackwell.

Cliff, A.D., Haggett, P., Stroup, D.F. & Cheney, E. (1992). The changing geographical coherence of measles morbidity in the United States, 1962–88. *Statistics Med.*, 11, 1409–1424.

Cliff, A.D., Haggett, P. & Smallman-Raynor, M. (1993). *Measles: An Historical Geography of a Major Human Viral Disease from Global Expansion to Local Retreat, 1840–1990.* Oxford: Blackwell.

Dietz, K. (1982). Overall population patterns in the transmission cycle of infectious agents. In *Population Biology of Infectious Diseases*, ed. Anderson R.M., May R.M. Berlin: Springer, pp. 87–102.

Earn, D., Rohani, P. & Grenfell, B.T. (1998). Spatial dynamics and persistence in ecology and epidemiology. *Proc. Roy. Soc. London, Ser. B*, 265, 7–10.

Ferguson, N.M., Nokes, D.J. & Anderson, R.M. (1996). Dynamical complexity in age structured models of the measles virus: epidemiological implications at high levels of vaccine uptake. *Mathemat Biosciences*, 138, 101–130.

Fine, P.E.M. & Clarkson, J.A. (1982). Measles in England and Wales – I: An analysis of factors underlying seasonal patterns. *Int. J. Epidemiol.*, 11, 5–15.

Finkenstädt, B.F. & Grenfell, B.T. (1998). Empirical determinants of measles metapopulation dynamics in England and Wales. *Proc. Roy. Soc. London, Ser. B*, 265, 211–220.

Finkenstädt, B.F., Keeling, M.J. & Grenfell, B.T. (1998). Patterns of density dependence in measles dynamics. *Proc. Roy. Soc. London, Ser. B*, 265, 753–762.

Greenwood, M., Bradford Hill, A.T., Topley, W.W.C. & Wilson, J. (1936). *Experimental Epidemiology.* Special Report: MRC.

Grenfell, B.T. (1992). Chance and chaos in measles dynamics. *J. Roy. Statist. Soc. Ser. B*, 54, 383–398.

Grenfell, B.T. & Dobson, A.P. (ed.) (1995). *Ecology of Infectious Diseases in Natural Populations.* Cambridge: Cambridge University Press.

Grenfell, B.T. & Harwood, J. (1997). (Meta) population dynamics of infectious diseases. *Trends Ecol. Evol*, 12, 395–399.

Grenfell, B.T., Kleczkowski, A., Ellner, S.P. & Bolker, B.M. (1994). Measles as a case-study in nonlinear forecasting and chaos. *Philosoph. Trans. Roy. Soc. London, Ser. a-Phys. Sci. Eng.*, 348, 515–530.

Grenfell, B.T., Bolker, B.M. & Kleczkowski, A. (1995). Seasonality and extinction in chaotic metapopulations. *Proc. Roy. Soc. London, Ser. B*, 259, 97–103.

de Jong, M.C.M., Diekmann, O. & Heesterbeek, J.A.P. (1995). How does transmission of infection depend on population size? In *Epidemic Models: Their Structure and Relation to Data*, ed. Mollison D. Cambridge: Cambridge University Press.

Keeling, M.J. & Grenfell, B.T. (1997). Disease extinction and community size: modeling the persistence of measles. *Science*, 275, 65–67.

Kermack, W.O. & MacKendrick, A.G. (1939). Contribution to the mathematical theory of epidemics. V – anaysis of experimental epidemics of mouse typhoid: a bacterial disease conferring incomplete immunity. *J. Hygiene (Cambridge)*, 39, 271–288.

May, R.M. & Anderson, R.M. (1984). Spatial heterogeneity and the design of immunization programs. *Math. Biosciences*, 72, 83–111.

May, R.M. & Anderson, R.M. (1985). Endemic infections in growing populations. *Math. Biosciences*, 77, 141–156.

Olsen, L.F., Truty, G.L. & Schaffer, W.M. (1988). Oscillations and chaos in epidemics: a nonlinear dynamic study of six childhood diseases in Copenhagen, Denmark. *Theoret. Population Biol.*, 33, 344–370.

Rhodes, C.J. & Anderson, R.M. (1996). Power laws governing epidemics in isolated populations. *Nature*, 381, 600–602.

Schenzle, D. (1984). An age-structured model of pre-and post-vaccination measles transmission. *IMA J. Mathematics Appl. Med. Biol.*, 1, 169–191.

BIOSKETCH

Bryan Grenfell works at the Zoology Department in Cambridge University, UK. He is interested in population dynamics in general, with special focus on the nonlinear dynamics and control of childhood infections; the immunoepidemiology of nematode infections; the evolution of anthelmintic drug resistance by parasitic nematodes; and sheep (population dynamics on St Kilda).